Influence of plasma instabilities on the propagation and spectrum of extragalactic electromagnetic cascades

Luis Enrique Espinosa Castro
Simone Rossoni
Günter Sigl

Universität Hamburg

CRPropa Workshop 2023

Contents

1. Very-high energy gamma-rays and electromagnetic cascades.
2. Effect of intergalactic magnetic fields.
3. Plasma instabilities and energy-losses.
4. Simulation of electromagnetic cascades, IGMF and plasma instabilities.
   Implementation of new CRPropa module for energy losses by instabilities.
5. Results and conclusions.

Motivation

- **Open problem:** suppression of photon flux observed for extragalactic gamma-ray sources.
- **Solution proposed:** deflections of electron-positron pairs beyond line-of-sight by intergalactic magnetic field.
- So far, bounds imposed on magnetic fields parameters based on observations.
- **Alternative:** plasma instabilities may change energy and momentum distribution of pairs, suppressing the cascade.
- In this work, a parametric study of energy losses by plasma instabilities was carried out.

Electromagnetic cascades

Electromagnetic interactions: pair production, inverse Compton scattering, double and triplet pair production

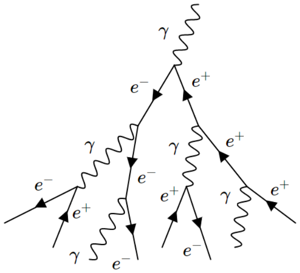

Figure: Scheme of electromagnetic cascade initiated by primary photon, depicting pair production and inverse Compton scattering stages.

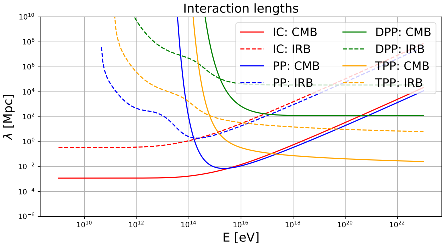

Figure: Interaction lengths of electromagnetic cascade processes as functions of incoming particle energy. For each process, interactions with the CMB and IRB, as modelled in (Franceschini et al, 2008), were considered.

IGMF: electron pair deflection

Effect quantified by deflection angle

$$\langle \theta^2 \rangle \sim \frac{L\lambda_c}{r_g^2}, \qquad r_g \sim \frac{E}{cqB_{rms}}$$

Then overall time delay of secondary photons can be related to a set of magnetic field parameters. (Neronov & Semikoz, 2009)

$$\tau = t_{pp} + t_\gamma - t_L \approx \frac{\lambda_{pp}\theta^2}{2c}\left(1 - \frac{\lambda_{pp}}{L}\right)$$

Thus, constraint can be made for magnetic field (for a certain observation time window).

$$\tau \approx 1.5 \cdot 10^3 \left(\frac{E}{10^{20}\,\mathrm{eV}}\right)^{-2} \left(\frac{L}{10\,\mathrm{Mpc}}\right)^2 \left(\frac{\lambda_c}{1\,\mathrm{Mpc}}\right) \left(\frac{B_{rms}}{10^{-9}\,\mathrm{G}}\right)^2 \mathrm{yrs}$$

Plasma instabilities

- Changes in electron density of plasma by passing electron beam creates oscillations of plasma.
- Interactions between cascade electron-positron pairs and plasma waves causes changes in momentum. (Alawashra & Pohl, 2022)
- General effect: angular broadening of cascade and energy losses of pairs. (Perry & Lyubarsky, 2021)
- Both effects reduce the number of secondary photons to be observed and, thus, suppress the photon flux at GeV energies.

Plasma instabilities

Energy-loss rates follow energy dependent power-laws $\tau \propto E^{\alpha}$. (Batista et al., 2019)

Select energy scale at which plasma instability energy-loss length and inverse Compton interaction length become comparable.

$\left(\lambda(E = \tilde{E}) = \lambda_{IC}(E = \tilde{E})\right)$ with $\lambda_{IC} = 1.2\,\mathrm{kpc}\,(1+z)^{-3}$ (Neronov & Semikoz, 2009)

One could set $\lambda_0 = \lambda_{IC}$, such that energy-loss lengths can be expressed as

$$\lambda(E) = \lambda_0 \left(\frac{E}{\tilde{E}}\right)^{\alpha}$$

$$\implies -\frac{dE}{dx} = \frac{\tilde{E}}{\lambda_0}\left(\frac{E}{\tilde{E}}\right)^{-\alpha+1}$$

Plasma instabilities

Variation of plasma instability energy-loss lengths for different values of plasma power index α and length scale λ_0. Inverse Compton scattering interaction length added for comparison.

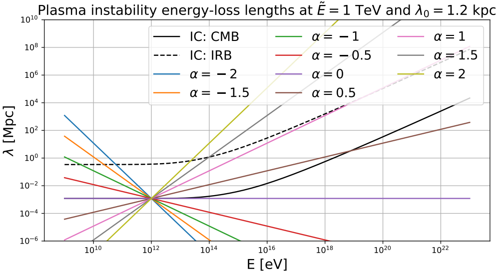

Figure: Plasma instabilities at $\tilde{E} = 1$ TeV and $\lambda_0 = 1.2$ kpc.

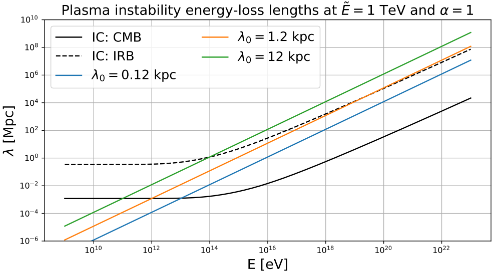

Figure: Plasma instabilities at $\tilde{E} = 1$ TeV and $\alpha = 1$.

Plasma instabilities

Dependence of energy losses on the distance for variations of plasma power index α and length scale λ_0 for a single electron of initial energy 1 TeV travelling 100 kpc.

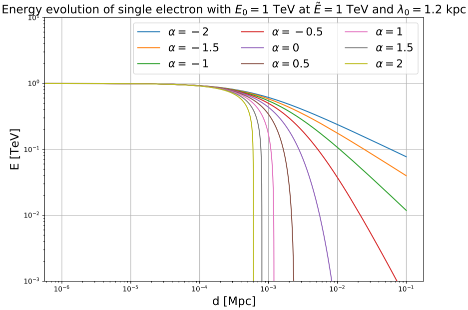

Figure: Plasma instabilities at $\tilde{E} = 1$ TeV and $\lambda_0 = 1.2$ kpc.

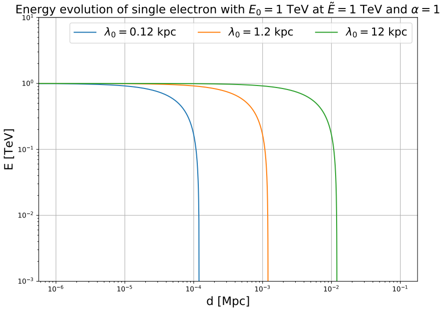

Figure: Plasma instabilities at $\tilde{E} = 1$ TeV and $\alpha = 1$.

Compute $F_c(E_\gamma, t) = \int_0^\infty \int_{E_\gamma}^\infty G(E_{\gamma,0}, E_\gamma, t-\tau, \tau) F_s(E_{\gamma,0}, t-\tau) dE_{\gamma,0} d\tau$ (Neronov et al., 2022)

Numerically, this is done by

$$J(E,t) = \sum_{t_0 \leq t} \sum_{E_0 \geq E} G(E_0, E, t_0, t) \cdot J(E_0, t_0)$$

To reconstruct detection flux for arbitrary emission of the form

$$J(E_0) = A \left(\frac{E_0}{1\ TeV} \right)^{-\beta} exp\left(-\frac{E_0}{E_{cut}} \right)$$

Results: role of plasma instabilities on detection spectra

Reconstructed spectra at Earth from an initial spectrum with $\beta = 1.2$ and $E_{cut} = 5$ TeV (1ES0229+200). Parametrization of instability energy losses with $\tilde{E} = 1$ TeV, $\alpha \in [-2, 2]$ and $\lambda_0 = 1.2$ kpc (left), $\lambda_0 = 0.12$ kpc (right).

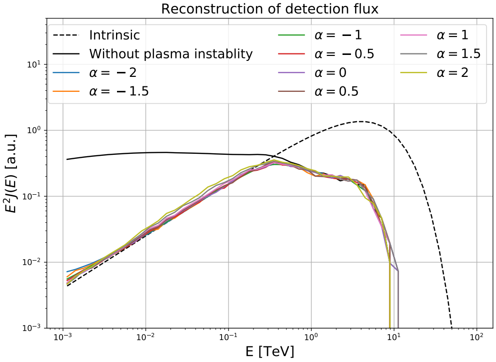

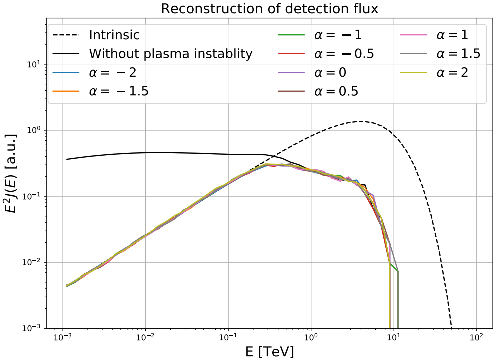

Results: role of plasma instabilities on detection spectra

Reconstructed spectra at Earth from an initial spectrum with $\beta = 1.2$ and $E_{cut} = 5$ TeV (1ES0229+200). Parametrization of instability energy losses with $\tilde{E} = 1$ TeV, $\alpha \in [-2, 2]$ and $\lambda_0 = 12$ kpc (left), $\lambda_0 = 120$ kpc (right).

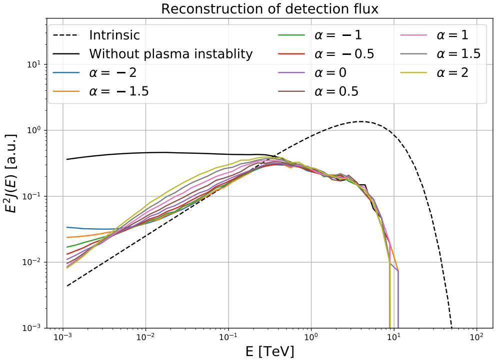

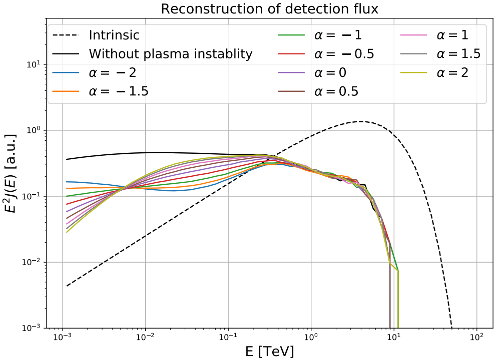

Results: variation of emission spectrum

Reconstructed spectra at Earth from initial spectra with $\beta = 1.9$, $E_{cut} = 1.3$ TeV (left) and $\beta = 1.2$, $E_{cut} = 2.5$ TeV (right). Parametrization of instability energy losses with $\lambda_0 = 12$ kpc, $\tilde{E} = 1$ TeV and $\alpha \in [-2, 2]$.

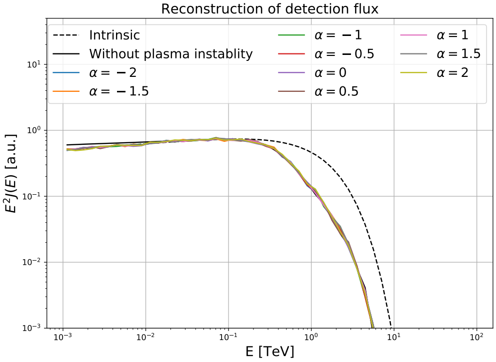

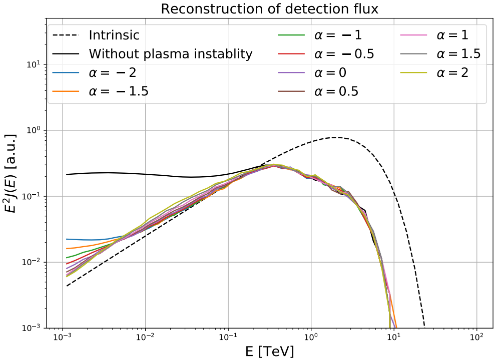

Results: time spectrum and cascade signal for inclusion of IGMF

Turbulent magnetic field with strength 10^{-17} G and correlation length 10^{-5} Mpc.

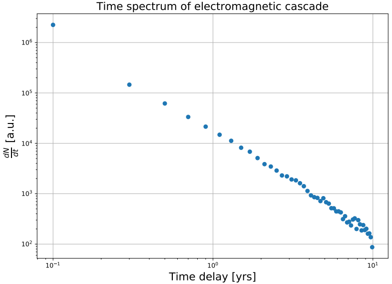

Figure: Time spectrum of the base CRPropa cascade simulation of 10^5 initial photons. Maximum delayed time set to 10 years.

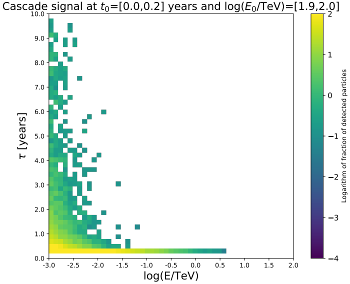

Figure: Example of cascade signal matrices for simulation of 10^5 initial photons. Color bar of the map is presented with logarithmic scale.

Results: comparison of plasma instabilities and IGMF

Reconstructed spectrum at Earth from a initial spectrum with $A = 1\,\text{TeV}^{-1}$, spectral index $\beta = 1.2$ and exponential cut-off at 5 TeV.
Magnetic field (blue line), plasma instabilities (color solid lines) and mixed scenarios (color dashed lines). Instabilities length scales: $\lambda_0 = 12$ kpc (orange), and $\lambda_0 = 120$ kpc (green) and $\lambda_0 = 1200$ kpc (red).

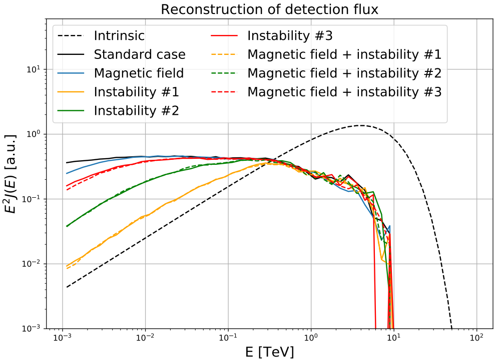

Conclusions and outlook

- Non-negligible role of suppression by plasma instabilities, even when they start to become subdominant.
- $\alpha < 0$ models present unique phenomenology and tend to show low energy-tails.
- Relative suppression dependent on emission spectral index.
- Comparable effect to IGMF for sufficiently high IGMF or plasma instability parameters.
- Lower bound the IGMF could undergo variations of some orders of magnitude.

- Future: setting upper and lower bounds on plasma parameters, addition of momentum-diffusion term, analysis of energetic prompt events (GRBs), plasma instability lab experiments.

References

- M. Alawashra, M. Pohl. The Astrophysical Journal. **929**. (2022).
- R. Alves Batista, A. Dundovic, M. Erdmann, K. H. Kampert, D. Kuempel, G. Müller, G. Sigl, A. van Vliet, D. Walz, T. Winchen. Journal of Cosmology and Astroparticle Physics. **2016**. (2016).
- R. Alves Batista, A. Savaliev, E. de Gouveia Dal Pino. Monthly Notices of the Royal Astronomical Society. (2019).
- A. Franceschini, G. Rodighiero, M. Vaccari. Astronomy and Astrophysics. **487**. (2008).
- C. Heiter, D. Kuempel, D. Walz, M. Erdmann. Astroparticle Physics. **102**. (2018).
- J. Jasche, A. van Vliet, J. P. Rachen. Proceedings of Science. (2019).

References

- S. Lee. Physical Review D. **58**. (1996).
- A. Neronov, D. Semikoz, A. Korochkin, MAGIC Collaboration. Astronomy and Astrophysics manuscript. **670**. (2022).
- A. Neronov, D. Semikoz. Physical Review D. **80**. (2009).
- R. Perry, Y. Lyubarsky. Monthly Notices of the Royal Astronomical Society. **503**. (2021).
- G. Sigl. Atlantis Studies in Astroparticle Physics and Cosmology. (2017).

Extra result: beyond time delay constraint

Reconstructed spectrum at Earth from a initial spectrum with $A = 1\,\text{TeV}^{-1}$, spectral index $\beta = 1.2$ and exponential cut-off at 5 TeV.
Magnetic field (blue line), plasma instabilities (color solid lines) and mixed scenarios (color dashed lines). Instabilities length scales: $\lambda_0 = 12$ kpc (orange), and $\lambda_0 = 120$ kpc (green) and $\lambda_0 = 1200$ kpc (red).